Available online at www.sciencedirect.com
SCIENCE DIRECT®
Polymer 45 (2004) 1533–1543
polymer
www.elsevier.com/locate/polymer

Amorphous-smectic glassy main chain LCPs. II. Dielectric study of the glass transition

A. García-Bernabé[a], R. Díaz Calleja[a,*], M.J. Sanchis[a], A. del Campo[b], A. Bello[b], E. Pérez[b]

[a]*Dept de Termodinamica Applicada, ETSII (UPV), Universidad di Politecnica/Valencia, Camino de Vera, Apartado 22012, Valencia 46022, Spain*
[b]*Instituto de Ciencia y Tecnología de Polímeros (C.S.I.C.), Madrid, Spain*

Received 8 April 2003; received in revised form 3 November 2003; accepted 17 December 2003

Abstract

The analysis of the dielectric relaxations of two main chain liquid crystalline polymers, derived from hydroxybibenzoic acid and (R,S)- and (R)-2-methyl-1,3-propanediol, is reported. These polymers can be obtained in their glassy amorphous, glassy liquid crystalline or in the crystalline state depending on their thermal history. The effect of the morphology of the sample on the dielectric spectra is analyzed. Particular interest has been paid to the characteristics of the dynamic glass transition of the different glassy states. It has been observed that the glass transition of the liquid crystalline SmC_{alt} phase occurs at lower temperatures and involves a smaller free volume than the glass transition of the amorphous fraction. The glass transition of the semicrystalline material follows the classical tendency of semicrystalline polymers.

Keywords: Dielectric relaxation; Polybibenzoate; Smectic glass

1. Introduction

Liquid crystalline polymers combine the characteristics of the liquid crystalline state with the specific properties of high molecular weight systems [1]. They exhibit anisotropy like conventional three-dimensional (3D) crystals, and an extensive polymorphism. They lack 3D long-range positional order like conventional fluids, being capable of flowing under stress. According to their macromolecular character, they have high mechanical stability and they are processable by different techniques. Their phase behaviour shows a strong dependence on the thermal history and they go through a glass transition by cooling. This combination of properties gives rise to a rich variety of phenomena. Among them, the possibility of freezing the orientational order of the mesophase just by cooling the sample at $T < T_g$ arises as an interesting way to obtain anisotropic glasses with unique optical, mechanical or electrical properties [2]. These effects have been extensively studied in side chain LCPs and elastomers.

In main chain liquid crystalline polymers the rigid groups are the building blocks of the macromolecular skeleton, the result of this geometry being a strong coupling of chain and mesogenic properties. The analysis of the polymeric behaviour in these systems must take into account special effects derived from the presence of orientational order, and therefore, it can show special characteristics differing from those found in classical amorphous polymers. Regarding the molecular dynamics of a LC polymer, an interesting point may be the study of the glass transition. Since the glass transition is related to the freezing of segmental motions, and liquid crystalline phases retain some mobility around the longitudinal axes of the mesogen, it seems reasonable to expect a glass transition of the liquid crystalline phase at the temperature at which the minimum free volume required for the rotations is approached. The glass transition temperature must be strongly related to the rotational freedom of the mesogens, which at the same time has to be compatible with the symmetry of the mesophase. In spite of the extensive interest in the solid state physics of LCPs, there are only a few examples in the literature dealing with the differences in the properties of the amorphous and liquid crystalline glasses of thermotropic main chain LCPs [3]. The existence of two different glass transitions for the liquid crystalline and amorphous states, the former laying at lower

* Corresponding author. Tel.: +34-9-6387-7320; fax: +34-9-6387-7329.
E-mail address: rdiazc@ter.upv.es (R. Díaz Calleja).

0032-3861/$ - see front matter © 2004 Elsevier Ltd. All rights reserved.
doi:10.1016/j.polymer.2003.12.073

temperatures than the latter, has been suggested by some authors regarding DSC and dielectric and dynamic–mechanic spectroscopy measurements [3,4]. However, deep studies in suitable systems remain undone.

In this work, a deep analysis of the relaxational behaviour of the glassy state of two semiflexible main chain LC polyestheresters has been performed. The polymers contain the biphenyl unit as mesogenic cores that are connected by 1-methyltrimethylene as substituted odd spacer. Ester and ether groups alternate as linking groups between the mesogen and the spacer along the polymeric chain. According to the configuration of the asymmetric center of the spacer, both the racemic (R,S-PBO3) and the enantiomerically pure (R-PBO3) polyetheresters were analyzed. The polymer structure, keeping in mind the random disposition of the spacer and the presence of a chiral center, can be depicted as:

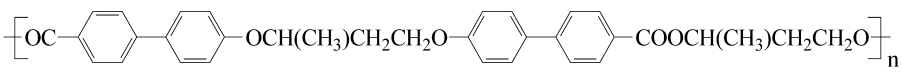

These systems have shown the ability to develop a SmC_{alt} and a crystalline mesophase depending on the stereochemistry of the asymmetric center and on the thermal treatment of the sample [5]. If the polymers are rapidly cooled from the melt at temperatures below the glass transition, the amorphous structure of the isotropic melt can be frozen. However, by annealing the samples at temperatures above the T_g, a liquid crystalline SmC_{alt} phase is slowly developed in the case of R,S-PBO3, and a crystalline phase in the case of R-PBO3. The extent of the transformation can be tuned by the annealing conditions and, therefore, samples where different morphologies coexist in different proportions can be analyzed. This analysis aims to help for the understanding of the molecular dynamics of the polymeric chain in the glassy liquid crystalline state in comparison to the molecular dynamics in the glassy amorphous state.

2. Experimental

The real and imaginary parts of the complex dielectric permittivity, ε' and ε'', were measured with a DEA 2970 apparatus (TA Instruments) in dry nitrogen atmosphere. The measurements were made in a temperature–sweep experiment at a heating rate of 1 °C min^{-1} over a temperature range from −130 to 80 °C and at frequencies between 10^{-1} and 10^5 Hz. From 80 °C to higher temperatures (about 200 °C), frequency multiplexing at 5 °C steps, was used. For each polymer, two samples with different thermal histories were analyzed: one was quenched from the melt and the other one was annealed previously during 12 h at a temperature of about 120 °C in R,S-PBO3 and 140 °C in the case of R-PBO3. The annealing was done in situ right before the beginning of the dielectric measurements.

3. Results

3.1. R,S-PBO3

The polyetherester R,S-PBO3 is a smectic main chain LCP that forms a SmC_{alt} mesophase due to the odd character of its flexible spacer [5]. The transformation of the isotropic melt into the smectic SmC_{alt} state occurs at very low formation rates, allowing the freezing of the sample into a supercooled amorphous glassy state at temperatures below the glass transition. By annealing this sample at a temperature above its glass transition for several hours, the SmC_{alt} phase is obtained. Controlling the annealing time and the annealing temperature, different degrees of transformation can be obtained, offering the possibility of a detailed analysis and comparison of the characteristics of the amorphous and the liquid crystalline glassy states. This analysis has been performed by dielectric spectroscopy. Fig. 1 shows the dielectric spectra of a quenched sample of R,S-PBO3 at three different frequencies (10^4, 10^2 and 1 Hz). Data are represented in terms of the dielectric permittivity and the loss factor. Two different relaxational

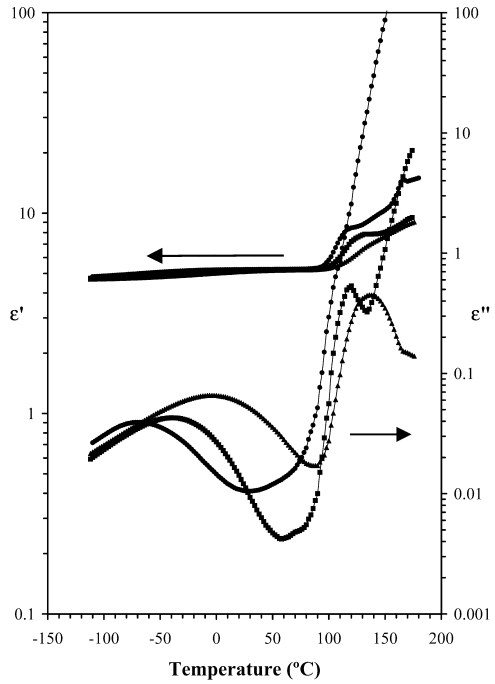

Fig. 1. Dielectric permittivity and loss for R,S-PBO3 before annealing experiment. (▲) 10^4 Hz, (■) 10^2 Hz and (●) 1 Hz.

zones can be clearly distinguished in the isochrones at 10^4 and 10^2 Hz: a broad, asymmetric and weak maximum extending from −100 to 80 °C, called β process, and a more intense, and narrower peak at higher temperatures. According to DSC data, the narrow relaxation (α process) has been attributed to the dynamic glass transition [5]. The maxima of the relaxations shift to higher temperatures when increasing the frequency of the measurement, as expected from the thermal activation of the molecular movements. Above 100 °C, an additional increase in ε'' with temperature is observed in the low frequency isochrones due to conductivity effects.

Fig. 2 shows analogous experiments obtained from a sample that has been annealed for 12 h at 120 °C. The experiments performed at low temperatures gave a similar profile to those of the quenched sample. However, at higher frequencies (spectrum recorded at 10^4 Hz), two partially overlapped peaks (instead of only one maximum) can be observed in the region of the α relaxation, one appearing at lower temperature and the other one at slightly higher temperature than the α relaxation of the amorphous sample. According to calorimetric results in a previous paper, this feature has been attributed to the coexistence of two molecular environments with different glass transition temperatures in the annealed sample [5]. The α peak detected at lower temperatures in the dielectric spectrum of the annealed sample is assigned to restricted segmental motion of the chains located in the liquid crystalline domains, and the one at higher temperatures to those in the amorphous regions. Segmental movement above the glass transition in the SmC_{alt} mesophase must be compatible with the orientational order, being therefore more restricted than in the amorphous state and appearing at lower temperatures.

In order to analyze the characteristic parameters of the different dipolar α-relaxations, the conductive contribution must be subtracted from the loss factor curve. In amorphous polymers, it is usual to assume a hopping conduction model, and the corresponding conductive contribution (ε''_c) can be fitted to the equation [6,7]:

$$\varepsilon''_c = \frac{\sigma}{\varepsilon \omega^s} \tag{1}$$

where σ is the conductivity, ε, permittivity of the free space, and ω, the angular frequency, s is a parameter whose value gives information about the physical origin of the conductivity. However, due to the structural complexity of our samples, the possible appearance of Maxwell–Wagner–Sillars (MWS) due to the phase boundaries can take place. A $\log \varepsilon''$ versus $\log \omega$ plot (Fig. 3) at high temperatures can be used to analyze this effect and eventually to determine the parameter s of Eq. (1). Values very close to the unity were found for s in all the cases, revealing that the conductivity is due to migration of free charges in the sample that are activated by the electric field at high temperatures and not to MWS or interfacial phenomena on the electrode–polymer interface. The activation energy of the conductive contribution is obtained plotting $\ln \sigma$ against T^{-1}, as shown in Fig. 4 where data corresponding to R-PBO3 are also presented. For the quenched sample of R,S-PBO3, a value of 169 kJ mol^{-1} was obtained at temperatures below the isotropisation temperature ($T_i = 149$ °C) and 138 kJ mol^{-1} at higher

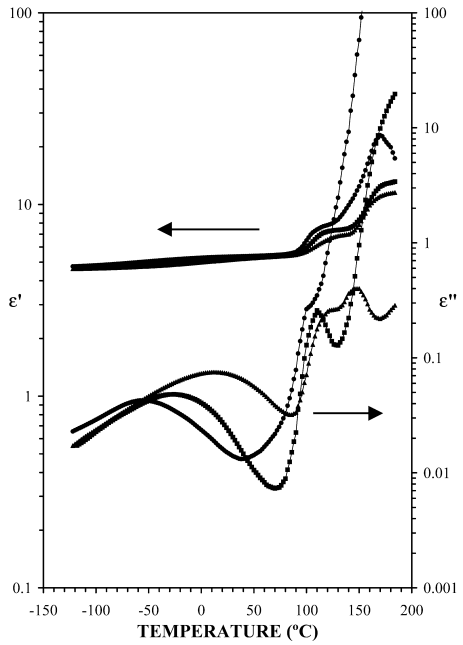

Fig. 2. Dielectric permittivity and loss for R,S-PBO3 after annealing experiment. (▲) 10^4 Hz, (■) 10^2 Hz and (●) 1 Hz.

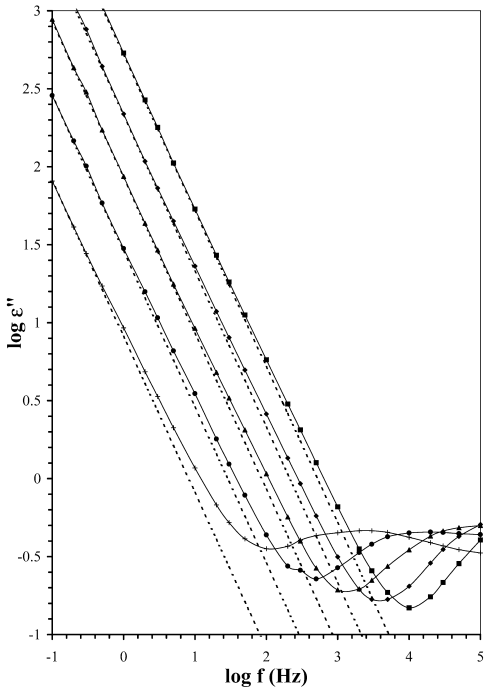

Fig. 3. Dielectric spectrum (loss permittivity) for R,S-PBO3 before annealing experiment. (+) 130 °C, (●) 140 °C, (▲) 150 °C, (◆) 160 °C, (■) 170 °C.

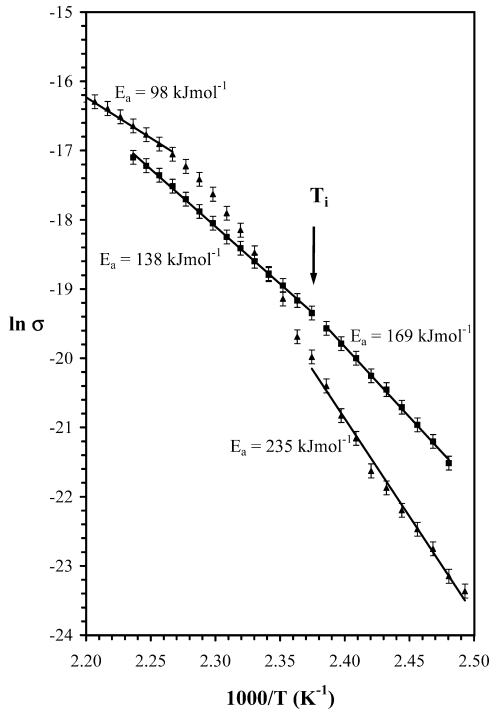

Fig. 4. Arrhenius plot for the conductivity of R,S-PBO3 ((■) quenched, (▲) annealed) and R-PBO3 ((◆) quenched,(●) annealed).

temperatures. The corresponding annealed sample showed a continuous variation of the activation energy from a value of 235 kJ mol^{-1} at temperatures below T_i to 98 kJ mol^{-1} at temperatures above T_i. In the common range of temperatures and between 165 and 175 °C, the activation energies of the quenched and annealed samples are nearly the same as corresponds to the isotropic state. These values are higher than expected and must be considered as apparent ones.

Once the conductive contribution was subtracted from the experimental results, the effect of the high temperature side of the broad β process must also be subtracted. We notice that the overlapping of α and β processes is only noticeable in the high frequency curves. Due to the asymmetric shape of the β process, it is assumed that this process is the result of two overlapping processes. Thus, the experimental curves was fitted to the addition of two Fuoss–Kirkwood (FK) equations according to the following scheme

$$\varepsilon'' = \sum_{i=1}^{2} \varepsilon''_{\max\, i}\, \mathrm{sech}\, \frac{m_i E_{ai}}{R}\left(\frac{1}{T} - \frac{1}{T_{\max\, i}}\right) \qquad (2)$$

where E_{ai} are the activation energies, $T_{\max\, i}$, the temperature of the maximum, and m_i, a shape parameter. The parameters of the fit are given in Table 1 where data corresponding to the four polymers analyzed are presented.

These values agree with other results known for flexible polyesters and they are of the same order of magnitude than those recently published for poly(triethylene glycol *p*,*p*′-bibenzoate-*co*-(*R*)-(+)3-methyl adipate) [8]. The Arrhenius prefactor is independent of the thermal history of the sample ($\ln(f_0) = 38$) and is equal to the Arrhenius prefactor of the β relaxation in poly(triethylene glycol *p*,*p*′-bibenzoate-*co*-(*R*)-(+)3-methyl adipate).

Then, the activation parameters of the dipolar α relaxations were analyzed. For the analysis of the α relaxation of the quenched sample, the Havriliak–Negami [9] equation was used:

$$\varepsilon^*(\omega) = \varepsilon_\infty + \frac{\varepsilon_0 - \varepsilon_\infty}{(1 + (i\omega\tau)^\alpha)^\beta} \qquad (3)$$

where ε_0 and ε_∞ are, respectively, the relaxed and unrelaxed dielectric permittivities, τ, the relaxation time and α and β are the parameters related to the shape and skewness of the complex dielectric plot. The fitting of the experimental data in the frequency domain to the semiempirical model was performed with the LEVM6 program [10]. Table 2 summarizes the Havriliak–Negami parameters at different temperatures calculated from the analysis of the α relaxation in the quenched sample. Surprisingly, the relaxation strength is found to increase with increasing temperature (see values of $\Delta\varepsilon$ in Table 2). This tendency was not expected, since the α process is considered to have a cooperative character, and cooperativity decreases with increasing temperature (the reorientation of a dipole is more and more influenced by its molecular environment when decreasing temperature). However, taking into account that the analyzed isotherms correspond to temperatures close to the glass transition, and that the dielectric measurements overall the frequency range require a long measuring time, a partial development of the liquid crystalline phase during the acquisition time might be the reason for the unexpected increase in $\Delta\varepsilon$. Cole–Cole plots showing the fit to HN equation for the quenched R,S-PBO3 sample, without subtracting conductive effects, are shown in Fig. 5. The presence of two α relaxations can be observed in a small, but noticeable, change of trend in the middle of the Cole–Cole plots (see arrows in Fig. 5).

The overlapping of the α peaks in the dielectric spectra of the annealed sample within the whole of frequency range accessible experimentally (see isothermal curves of Fig. 6) hinders the analysis of the α relaxation by a simple Havriliak–Negami equation. In order to obtain additional information about the origin of these complex structures, isothermal experiments were performed at different annealing times at 120 °C. The measurements after annealing times between 30 and 720 s are shown in Fig. 7. At the beginning of the annealing experiment, only one relaxational process can be distinguished and should be related to the amorphous phase. When the annealing time increases, the intensity of this process decreases and, at the same time, another broad process at higher frequencies appears, in a parallel way to the development of the liquid crystalline phase. The half width of this new peak is two or three times larger than those corresponding to a single α peak. For this reason, its broadness is interpreted as the presence of two

Table 1
Parameters of Fuoss–Kirkwood equation for β relaxation of

f (Hz)	$\varepsilon''_{max}(1)$	$T^{(1)}_{max}$ (°C)	$m^{(1)}$	$\Delta\varepsilon^{(1)}$	$\varepsilon''_{max}(2)$	$T^{(2)}_{max}$ (°C)	$m^{(2)}$	$\Delta\varepsilon^{(2)}$
(a) RS-PO3 before annealing experiment								
5×10^4	0.067	28	0.25	0.537	0.034	−55	0.06	1.171
3×10^4	0.062	23	0.27	0.464	0.035	−56	0.07	1.029
2×10^4	0.059	18	0.27	0.444	0.033	−58	0.07	0.921
1×10^4	0.054	12	0.26	0.407	0.030	−62	0.07	0.797
5×10^3	0.042	−8	0.21	0.406	0.030	−71	0.08	0.748
3×10^3	0.036	−12	0.21	0.352	0.029	−68	0.08	0.713
2×10^3	0.036	−15	0.21	0.349	0.028	−71	0.09	0.655
1×10^3	0.034	−20	0.21	0.322	0.027	−74	0.09	0.605
$E_a^{(1)} = 76.70\ kJ\ mol^{-1}$; $E_a^{(2)} = 70.59\ kJ\ mol^{-1}$								
(b) RS-PO3 after annealing experiment								
5×10^4	0.067	28	0.252	0.532	0.034	−55	0.059	1.171
3×10^4	0.062	23	0.267	0.464	0.035	−56	0.068	1.029
2×10^4	0.059	18	0.267	0.442	0.033	−58	0.072	0.921
1×10^4	0.054	12	0.264	0.409	0.03	−62	0.074	0.797
5×10^3	0.0508	6	0.238	0.427	0.0323	−66	0.083	0.778
3×10^3	0.0469	2	0.256	0.366	0.0313	−67	0.094	0.666
2×10^3	0.0485	−2	0.254	0.382	0.0308	−72	0.103	0.598
1×10^3	0.0456	−7	0.263	0.347	0.0294	−76	0.11	0.535
$E_a^{(1)} = 74.31\ kJ\ mol^{-1}$; $E_a^{(2)} = 66.82\ kJ\ mol^{-1}$								
(c) R-PO3 before annealing experiment								
1×10^5	0.0316	16	0.19	0.334	0.0277	−45	0.07	0.749
5×10^4	0.0316	9	0.18	0.342	0.0205	−62	0.10	0.404
3×10^4	0.0290	4	0.18	0.314	0.0187	−62	0.10	0.361
2×10^4	0.0280	1	0.19	0.291	0.0180	−65	0.12	0.303
1×10^4	0.0239	−6	0.20	0.237	0.0172	−61	0.12	0.279
5×10^3	0.0244	−10	0.20	0.243	0.0176	−73	0.13	0.267
3×10^3	0.0229	−15	0.20	0.228	0.0163	−74	0.14	0.237
2×10^3	0.0214	−19	0.20	0.219	0.0157	−73	0.13	0.250
5×10^2	0.0217	−28	0.19	0.224	0.0138	−88	0.15	0.184
$E_a^{(1)} = 81.17\ kJ\ mol^{-1}$; $E_a^{(2)} = 40.73\ kJ\ mol^{-1}$								
(d) R-PO3 after annealing experiment								
2×10^4	0.0345	−5	0.25	0.271	0.0228	−73	0.12	0.395
1×10^4	0.0312	−12	0.26	0.237	0.0203	−74	0.12	0.326
5×10^3	0.0326	−16	0.27	0.239	0.0219	−78	0.15	0.297
2×10^3	0.0252	−23	0.25	0.198	0.0186	−76	0.12	0.307
1×10^4	0.0241	−29	0.25	0.189	0.0167	−82	0.12	0.274
5×10^2	0.0225	−37	0.25	0.180	0.0149	−90	0.10	0.305
$E_a^{(1)} = 62.68\ kJ\ mol^{-1}$; $E_a^{(2)} = 62.22\ kJ\ mol^{-1}$								

Table 2
Parameters of the Havriliak–Negami equation for R,S-PBO3 before annealing experiment

T (°C)	ε_0	ε_∞	$\Delta\varepsilon$	α	β	τ (s)
116	7.93	5.18	2.75	0.81	0.26	1.92×10^{-2}
118	8.02	5.14	2.88	0.76	0.26	1.12×10^{-2}
120	8.10	5.13	2.97	0.73	0.28	6.08×10^{-3}
122	8.24	5.18	3.06	0.57	0.39	2.84×10^{-3}
124	8.25	5.16	3.09	0.52	0.43	1.40×10^{-3}

overlapping relaxations The conductive contribution decreases with increasing annealing time due to the hindered movement of free charges across the LC phase. Unfortunately, the frequency range experimentally available was not enough to distinguish the two relaxational processes either, and a more detailed real time evolution study during the annealing was not possible. However, it is possible to deconvolute the two observed peaks in the high frequency isochronal data of Fig. 2 by using two HN equations [11]. Typical curves at 30 kHz are shown in Fig. 8, where the confidence limits are also shown. The corresponding parameters are presented in Table 3.

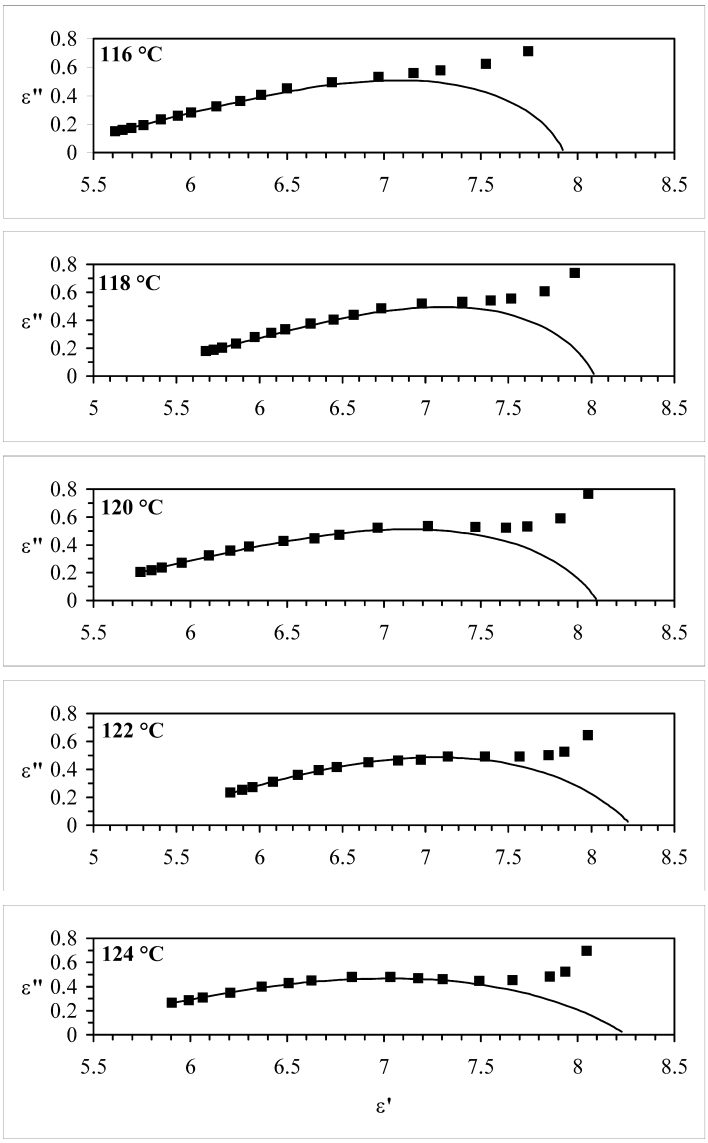

Fig. 5. Cole–Cole plots of quenched R,S-PBO3 at several temperatures.

The temperature dependence of the two α relaxations was analyzed by means of the Vogel–Fulcher–Tamman–Hesse [12–14] (VFTH) equation based on the free volume theory:

$$\ln f_{\max} = A - \frac{m}{T - T_\infty} \tag{4}$$

where A and m are constants and T_∞ in this equation is an empirical parameter related to the Kauzmann temperature or the temperature at which the conformational entropy is zero.

The comparison of VFTH equation with the Doolittle [15,16] equation yields

$$\frac{\phi}{B} = \frac{T - T_\infty}{m} \tag{5}$$

which relates the free volume in the Doolittle equation ϕ,

Table 3
Parameters of the deconvolution of isochrones in the α zone of R,S-PBO3

f (Hz)	$\Delta\varepsilon^{(1)}$	$m^{(1)}$	$T_c^{(1)}$ (°C)	$\alpha^{(1)}$	$\beta^{(1)}$	$\Delta\varepsilon^{(2)}$	$m^{(2)}$	$T_c^{(2)}$ (°C)	$\alpha^{(2)}$	$\beta^{(2)}$
5×10^4	2.086	2115.8	126.7	0.25	0.87	1.925	2076.7	161.1	0.58	0.63
3×10^4	2.085	2195.8	124.6	0.25	0.87	1.781	2092.6	156.5	0.56	0.71
2×10^4	2.061	2260.5	123.7	0.26	0.82	1.761	2170.7	154.6	0.56	0.65
1×10^4	2.050	2489.0	120.3	0.26	0.83	1.641	2052.3	152.5	0.57	0.61

$T_\infty^{(1)} = 47$ °C; $T_\infty^{(2)} = 52$ °C.

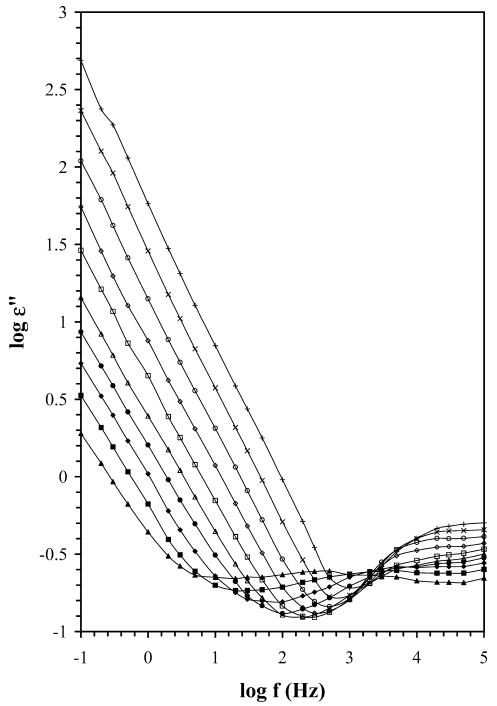

Fig. 6. Dielectric spectrum (loss permittivity) for R,S-PBO3 after annealing experiment. (▲) 114 °C, (■) 118 °C, (◆) 122 °C, (●) 126 °C, (△) 130 °C, (□) 134 °C, (◇) 138 °C, (○) 142 °C, (×) 146 °C and (+) 150 °C.

with the values of m in Eq. (4). From the values of m, the relative free volume at T_g, (ϕ_g/B), can be obtained. These equations were applied to the experimental data. The temperature dependence of the α relaxations of the different maxima associated with the amorphous and the LC phases in the annealed and quenched samples are shown in Fig. 9. Although the assignation of a glass transition temperature to the liquid crystalline phase remains somehow questionable, the temperature dependence of all the peaks follows undoubtedly a VFTH dependence. The values obtained for the relevant parameters are shown in Table 4. The relative

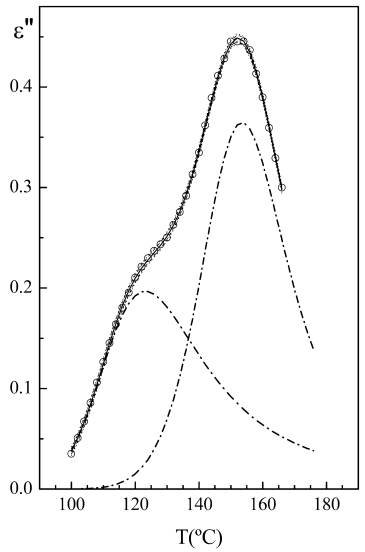

Fig. 8. Splitting of the two observed α peaks in the isochrones at 30 kHz.

Table 4
Parameters of the VFTH equation and relative free volume

	R,S-PBO3 (annealed sample)		R-PBO3	
	Amorphous	SmC_{alt}	Amorphous (quenching)	3D-ordered (annealed)
m	2033	2241	1868	2005
T_∞ (°C)	52	47	48	32
T_g (°C)	104	98	98	98
Φ_g/B (%)	2.55	2.28	2.78	3.36
$E_{a\beta}$ (kJ mol^{-1})	269	294	260	256

free volume ϕ_g/B amounts 2.28% (assuming $T_g = 98$ °C) and 2.55% (assuming $T_g = 104$ °C) in the liquid crystal and amorphous phases of the annealed sample, respectively. These values are in good agreement with the free volume theory. It is noticeable that the LC phase presents not only a

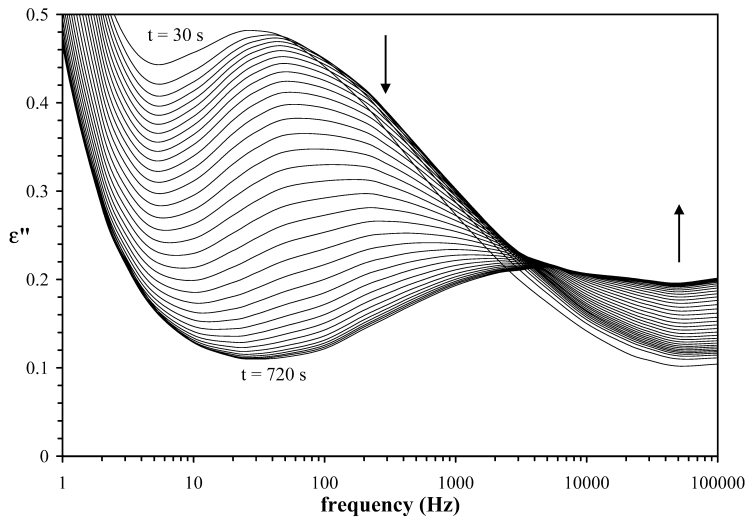

Fig. 7. Evolution of loss permittivity for R,S-PBO3 with the time at 120 °C. The first measured is realized at 30 s and the last at 720 s.

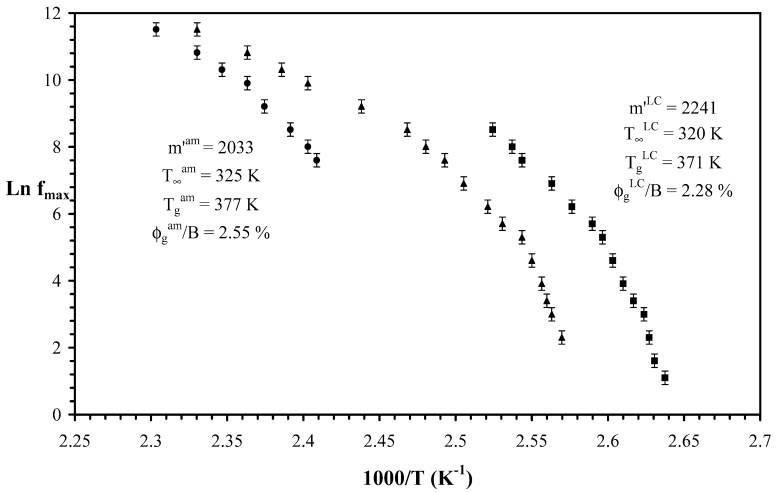

Fig. 9. Plot of log f against $10^3/T$ for the α relaxations of R,S-PBO3 showing the parameters of the free volume theory. (■) Amorphous phase and (◆) liquid crystal phase after annealing experiment. (▲) before annealing experiment.

lower glass transition temperature than the amorphous phase, but needs also a smaller free volume to be activated. The molecular rotations giving rise to the absorption in the LC phase seems to need a smaller room to be performed. The temperature dependence of the α relaxation in the quenched sample shows a mixed behaviour, halfway between that of amorphous and that of liquid crystalline phase.

3.2. R-PBO3

In a similar way to R,S-PBO3, the enantiomerically pure polyetherester can be obtained in its amorphous glassy state. Annealing experiments at temperatures above the glass transition for a given time also lead to the development of an ordered structure [5]. In this case, the ordered phase is not a 2D-smectic mesophase, but shows 3D-symmetry. The higher configurational symmetry of the R-PBO3 chain, due to the presence of only one of the two possible enantiomers of the chiral center, must be the reason for the formation of a mesophase of a higher order than the SmC_{alt} mesophase formed by the racemic polymer R,S-PBO3 [5, 17].

Figs. 10 and 11 show the dielectric permittivity and loss as a function of the temperature for the quenched and annealed samples of R-PBO3. As in R,S-PBO3, there are two relaxational regions: a broad and weak β process at low temperatures, and a more intense and narrower (α peak together with the conductive contribution at higher temperatures. A spurious peak, probably due to conductive effects, appears in the quenched sample (see Fig. 10, 1 Hz curve at about 125 °C). The apparent activation energy for the conductive process is 156 kJ mol^{-1} in the quenched sample and 201 kJ mol^{-1} in the annealed sample (Fig. 4). The β relaxations have been analyzed in the same way as in the case of R,S-PBO and the corresponding parameters are also shown in Table 1. The values obtained for R-PBO3 are similar to those calculated for R,S-PBO3.

The α process is detected at higher temperatures as a single peak in both samples. However, the α peak of the annealed sample is broader, has a lower intensity and is shifted to slightly higher temperatures when compared with that of the amorphous sample. The annealing process in this case does not lead to separated domains with different glass transition temperatures, at least within the resolution of the dielectric spectrum, but to a hindering of the molecular dynamics behind the transition. The lower intensity and the shift to higher temperatures of the peak is associated to the

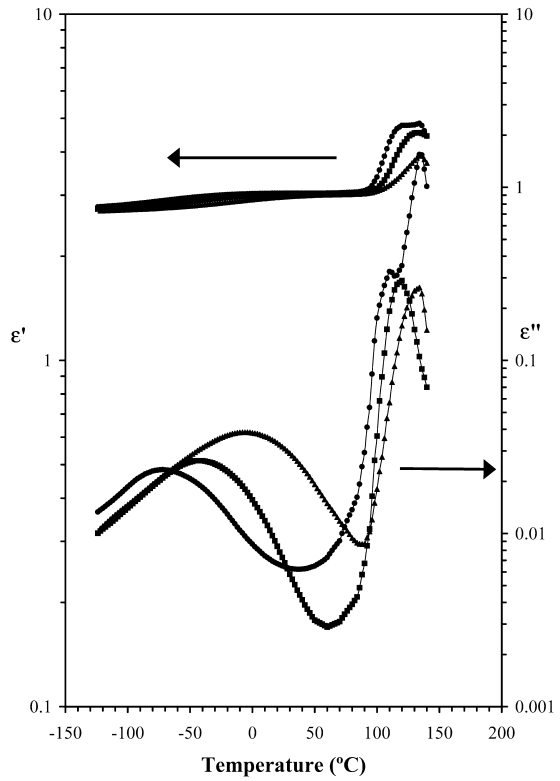

Fig. 10. Dielectric permittivity and loss for R-PBO3 before annealing experiment. (▲) 10^4 Hz, (■) 10^2 Hz and (●) 1 Hz.

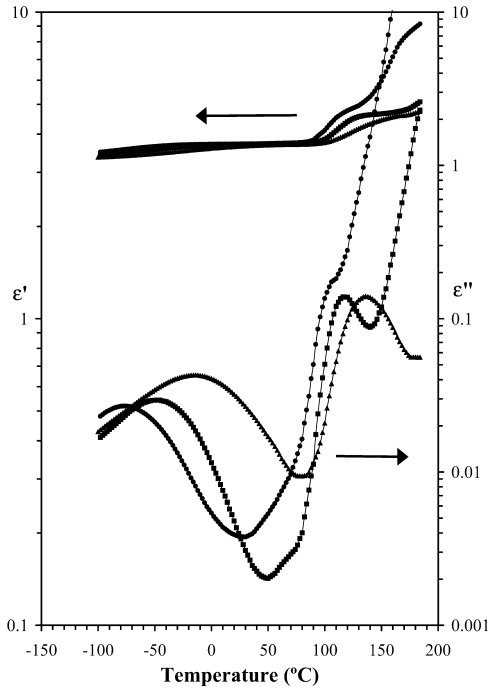

Fig. 11. Dielectric permittivity and loss for R-PBO3 after annealing experiment. (▲) 10^4 Hz, (■) 10^2 Hz and (●) 1 Hz.

movements of the chains in the remaining amorphous fraction, which becomes partially hindered through the confinement of the amorphous domains between the ordered domains. This situation has been also observed in the annealing process of polyethylene-terephtalate that leads to a partially crystallized material [18].

The parameters of the α relaxation in the amorphous and annealed samples were analyzed according to the Havriliak–Negami model. The calculated values for different parameters are summarized in Tables 5 and 6. In both quenched and annealed samples, the relaxation strength increases with the temperature, in the same way as it was found in the quenched R,S-PBO3. Again, this feature can be interpreted as an indication of the coexistence of crystalline and amorphous phases. Cole–Cole plots for quenched and annealed samples of R-PBO3 without subtracting conductivity, are shown in Fig. 12. The temperature dependence of α relaxations seems to follow also a VFTH behaviour, as shown in Fig. 13. Although the

Table 5
Parameters of the Havriliak–Negami equation for R-PBO3 before annealing experiment

T (°C)	ε_∞	ε_0	$\Delta\varepsilon$	α	β	τ (s)
118	3.01	4.41	1.40	0.86	0.25	0.0044
120	2.97	4.49	1.51	0.89	0.23	0.0033
122	2.92	4.47	1.55	0.91	0.21	0.0020
124	2.85	4.50	1.65	0.89	0.19	0.0014
126	2.79	4.53	1.74	0.87	0.19	0.0010

Table 6
Parameters of the Havriliak–Negami equation for R-PBO3 after annealing experiment

T (°C)	ε_∞	ε_0	$\Delta\varepsilon$	α	β	τ (s)
118	3.61	4.46	0.85	0.70	0.21	0.0028
120	3.61	4.53	0.92	0.63	0.25	0.0023
122	3.60	4.59	0.99	0.56	0.28	0.0019

use of the free volume theory for a semicrystalline material is questionable, the values of the different parameters were calculated and are given in Table 4. Values of 2.78 and 3.36 were obtained for ϕ_g/B in the quenched and annealed sample, respectively. In the case of the quenched sample, the value is slightly higher than the one obtained for the racemic polymer. The value obtained for the annealed sample is slightly higher than the values predicted by the free volume theory.

4. Discussion

The polymers derived from 4,4′-hydroxybibenzoic acid and (R)- or (R,S)-2-methyl-1,3-propanediol are main chain polyetheresters with a very slow rate of formation of the mesophases. This particular property is due to their chemical structure, containing geometrical and structural disruptions of the molecular symmetry that hinder the ordering processes. On the other hand, the introduction of a flexible spacer with an odd number of carbons induces an antiparallel disposition of consecutive mesogens that hinders the packing of the chains. On one hand, the presence of a lateral methyl group in a short spacer and in a position close to the mesogen group may cause also a strong distortion in the packing. These facts allow the freezing of the sample into the homogeneous amorphous state, and therefore, the comparison of the dynamics of the chain in the amorphous and in the liquid crystalline environment. Besides that, different degrees of transformation can be obtained by controlling the annealing time, opening the possibility of a detailed analysis of the characteristics of the dielectric relaxations in both states.

The presence of a lateral methyl group in the spacer also generates another possibility of tuning the transitional properties of the polymer by changing the stereochemistry of the substituted carbon. This effect is reflected in the different phase sequence obtained for the polymers R,S-PBO3 and R-PBO3. The racemic polymer, R,S-PBO3, forms upon annealing a low ordered SmC_{alt} phase, whereas the enantiomerically pure polymer, R-PBO3, forms a crystalline phase. These differences in their phase sequence are also reflected in the dielectric properties of the systems. In particular, the dynamic glass transition undergoes strong changes depending on the morphology of the sample.

Attending to the calorimetric and dielectric experimental evidences, two different glass transitions have been detected

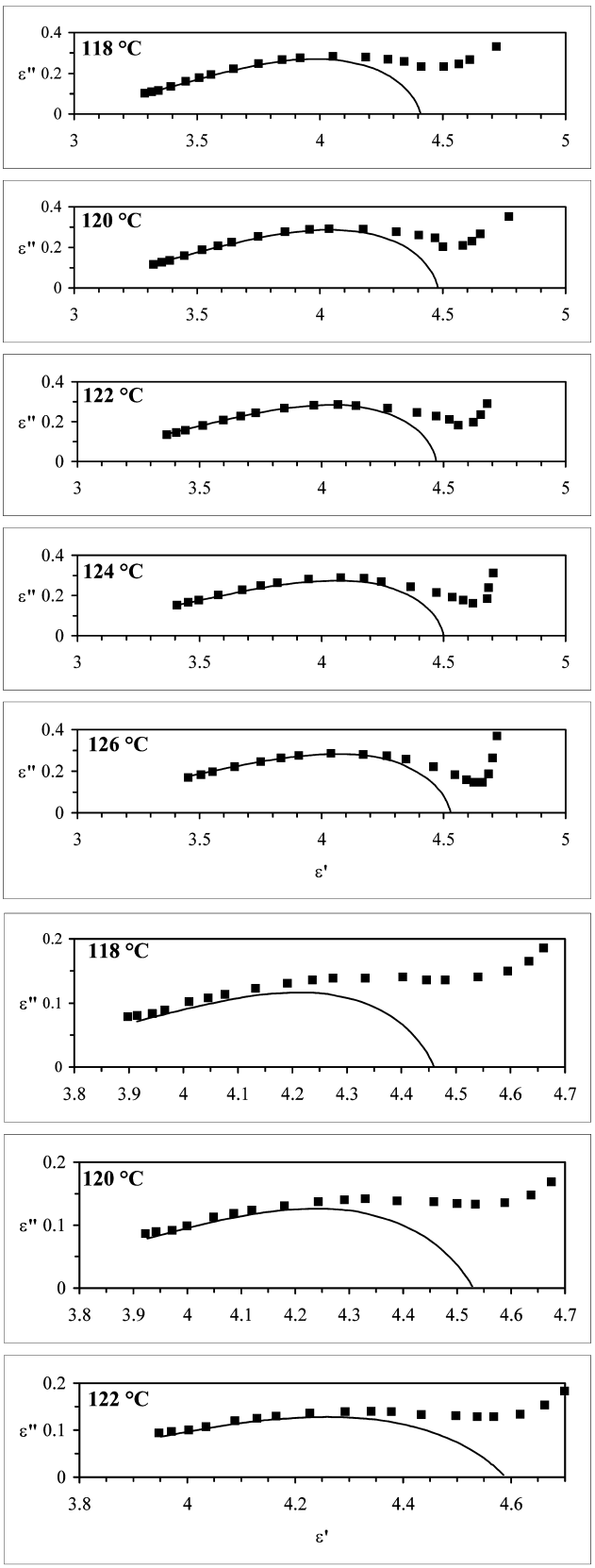

Fig. 12. Cole–Cole plots corresponding to quenched and annealed R-PBO3.

and associated to the amorphous and SmC_{alt} phases of R,S-PBO3 [5]. According to the classical theory, the glass transition temperature of polymers is closely related to the flexibility of the chains in the sense that a high value of T_g is generally assumed to be connected with relatively high barriers of bond rotations. These barriers depend not only on the type of bond, but also on the intermolecular constraint and, therefore, on the supramolecular arrangement of the chains. For this reason, a different location of the glass transition temperature of the liquid crystalline phase and that of the amorphous phase is not surprising. The polyetherester R,S-PBO3 constitutes, as far as we know, the first example of main chain LCP where the formation rate of its mesophase is sufficiently slow to allow the freezing of the sample into the homogeneous amorphous state and, therefore, to detect the glass transition of the glassy liquid crystalline and the glassy amorphous phases.

The glass transition of the SmC_{alt} phase seems to be activated at lower temperatures and seem to involve a smaller free volume than the glass transition of the amorphous phase. These results seem to be also in accordance with the free volume theory. Conformational analysis and X-ray diffraction indicate that highly extended conformers predominate in the LC phase [7]. Segmental movement above the glass transition in the LC phase shall not modify this orientation significantly, being therefore more restricted than in the amorphous state. The free volume necessary to perform these rotations is considerably smaller than the volume for segmental motion in the isotropic melt. Consequently, the glass transition of a LC phase should be reached at lower temperatures and should involve smaller free volumes than the glass transition of the isotropic state [4].

The dielectric behaviour of the dymamic glass transition of the annealed sample of R-PBO3, forming a 3D ordered phase, follows the same tendencies observed for classical semicrystalline polymers. The loss of intensity and the shift to higher temperatures of the α relaxation upon an annealing is associated to the movements of the chains in the remaining amorphous fraction, which becomes partially hindered through the confinement of the amorphous domains between the crystallites

The complex secondary β relaxation does not show a significant change with the morphology of the sample. Neither the extent of the transformation, nor the type of mesophase that it is formed has an influence on the position or activation energy of the relaxation. Taking into account the frequency, the temperature range, and the calculated activation energy, and comparing them with previous results published in the literature for other polymers [19], this process is associated with the rotation of the mesogens around their longitudinal axes coupled with motions in the flexible spacer. The polar linking groups between the mesogen and the flexible spacer also participate in the phenyl ring flips, making them detectable by dielectric spectroscopy. The independence of the local motions

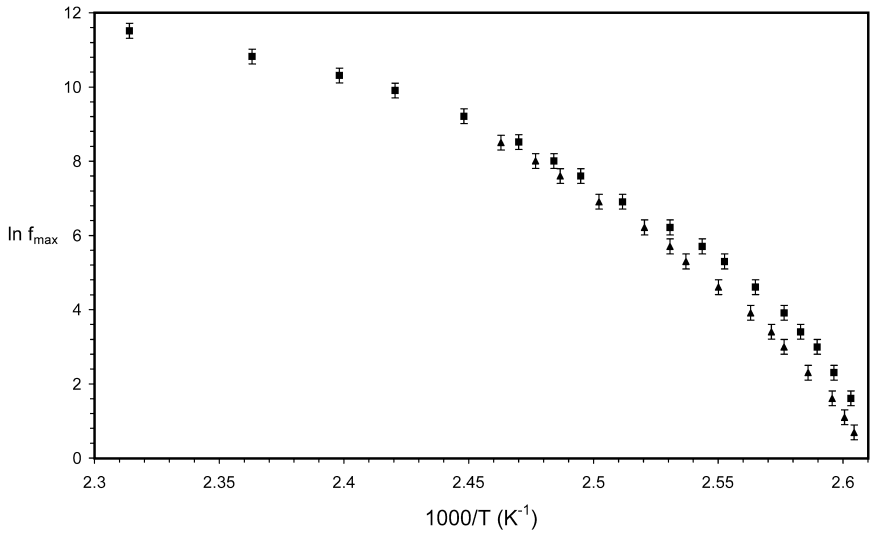

Fig. 13. Plot of $\log f$ against $10^3/T$ for the α relaxations of R-PBO3. (▲) quenched sample and (■) annealed sample.

responsible for the sub-glass relaxations on the morphology of the sample has also been observed in other studies on the dielectric properties of crystalline polymers [20].

5. Conclusions

Dielectric spectroscopy seems to be an useful tool in order to elucidate the fine structure of the α relaxational zone of R,S-PBO3. However, it is not possible to analyze in the same way the complex α relaxation of R-PBO3. In this case, only the broadening and the shift of the peak to higher temperatures seems to be an indication of the presence of ordered domains coexisting with the amorphous phase. It is noticeable that conductive effects contaminate the high temperature side of the isochrones giving rise in some case to spurious peaks. On the other hand, the β relaxation of the two polymers under study, appears to be not affected by the changes in the morphology.

Acknowledgements

R. Díaz-Calleja and M.J. Sanchis thanks to CICYT for Grant MAT2002-04042-C02-01 and MAT 2001-1731.

References

[1] Greiner A, Schmidt HW. In: Demus D, Goodby J, Gray GW, Spiess HW, Vill V, editors. Handbook of liquid crystals, vol. 3. New York: Wiley-VCH; 1998.
[2] Brand HR, Finkelmann H. In: Demus D, Goodby J, Gray GW, Spiess HW, Vill V, editors. Handbook of liquid crystals, vol. 3. New York: Wiley-VCH; 1998.
[3] Frosini V, de Petris S, Chiellini E, Galli G, Lenz RW. Mol Cryst Liq Cryst 1983;98:223. Gómez MA, Marco C, Fatou JMG, Suárez N, Laredo E, Bello A. J Polym Sci, Part B: Polym Phys 1995;3:1259. Tokita M, Osada K, Watanabe J. Polym J 1998;30:589.
[4] Chen D, Zachmann HG. Polymer 1991;32:1612. Ahumada O, Ezquerra TA, Nogales A, Baltá-Calleja FJ, Zachmann HG. Macromolecules 1996;29:5002.
[5] del Campo A, Bello A, Pérez E, Garcia-Bernabé A, Díaz-Calleja R. Macromol Chem Phys 2002;203:2508.
[6] Díaz-Calleja R, Riande E, San Román J, Compañ V. Macromolecules 1995;28:614.
[7] Boyd RH, Liu F. In: Runt JP, Fitzgerald JJ, editors. Dielectric spectroscopy of polymeric materials. Washington, DC: ACS; 1997.
[8] Garcia-Bernabé A, Díaz-Calleja R, Bello A, Pérez E. Polymer 2001; 42:6793.
[9] Havriliak S, Negami S. Polymer 1967;8:161.
[10] Macdonald JR. Complex non linear least squares immitance fitting program LEVM6. Department of Physics and Astronomy, University of North Carolina; 1993.
[11] Shlosser E, Schönhals A, Carius HE, Goering H. Macromolecules 1993;26:6027.
[12] Vogel H. Z Phys 1921;22:645.
[13] Fulcher GS. J Am Ceram Soc 1925;8:339.
[14] Tamman G, Hesse W. Z Anorg Allergy Chem 1926;156:245.
[15] Doolittle AK. J Appl Phys 1951;22:1471.
[16] Doolittle AK. J Appl Phys 1952;23:236.
[17] Pérez E, del Campo A, Bello A, Benavente R. Macromolecules 2000; 33:3023.
[18] Coburn JC, Boyd R. Macromolecules 1986;19:2238.
[19] Avakian P, Coburn JC, Connolly MS, Sauer BB. Polymer 1996;37: 3843. Gedde UW, Liu F, Gustafsson A, Jonsson H, Boyd RH. Polymer 1991;32:1219.
[20] McCrum NG, Read BE, Williams G. Aneslatic and dielectric effects in polymeric solids, 1967. New York: Dover; 1991. Reprint.